Ceramics-Silikáty 64 (4), 398-406 (2020)
www.ceramics-silikaty.cz doi: 10.13168/cs.2020.0027

IMPROVEMENT OF CEMENT PASTES COMPOSITE PROPERTIES CONTAINING CLAY NANOPARTICLES

#MOHAMED HEIKAL*, **, IVON M. HELMY***, SHEREEN AWAD****, NOHA S. IBRAHIM***, ****

*Chemistry Department, Faculty of Science, Benha University, Benha, Egypt
**Chemistry Department, College of Science, Imam Mohammad Ibn Saud Islamic University (IMSIU), P.O Box 90950, Riyadh 11623, Saudi Arabia
***Chemistry Department, Faculty of Science, Zagazig University, Zagazig, Egypt
****Faculty of Engineering, Benha University, Benha, Egypt

#E-mail: mohamed.heikal@fsc.bu.edu.eg

Submitted April 1, 2020; accepted May 7, 2020

Keywords: Clay nanoparticles, FA, FBFS, Hydration characteristics, Compressive strength

The present work aims to investigate the influence of clay nanoparticles (CNP) on the mechanical, physical and microstructure cement pastes composites. The cement paste composites were formulated by adding 20-60 mass % fly ash (FA), fine blast furnace slag (FBFS) and/or 6 mass % clay nanoparticles. The physico-chemical properties of the cement paste composites (CPC) were improved by the substitution of 6 % CNP in instead of OPC (ordinary Portland cement) in the consistence of the superplasticiser (SP). The physico-mechanical properties and hydration characteristics were investigated by the determination of the setting times (STs), the consistency (W/C, %), the free lime (FL), the combined water (Wn), the gel/space ratio (X), the total porosity (TP), the compressive strength (CS) and the bulk density (BD). The compressive strength values of the cement-CNP hybrid were higher than those of the cement paste composites without CNP. The STs of CPC-pastes containing CNP were accelerated. The CNP showed synergetic effect with the FA and FBFS to enhance the performance of pozzolanic reaction to form supplementary CSH, CAH and CASH, these phases are responsible for bridging, producing a rigid closed compact structure; hence the compressive strength, gel/space ratio, bulk density and chemically combined water increased, whereas the porosity decreased.

INTRODUCTION

Nowadays, the construction industry is mainly based on advanced concrete and modified cement paste composites, this is attributed to their, good performance, versatile applications easiness to fabricate, and low expenditure. However, the disadvantages of these cement-based materials, such as their low tensile strength, have led to multiple pathways of degradation in the technical properties of cement-based materials and the high costs of repairing them [1]. Recently, nano-materials were used to enhance all the properties and durability performances of modern concrete. It was shown that adding nano-materials may enhance the properties due to its surface effect, size effect, and interface effect. Nano-materials (NMs) affect the performance of the physico-mechanical, chemical and microstructure of the cement composite by nucleation, seeding and filler effect. These materials facilitate the pozzolanic reaction to form C–S–H, CAH, and CASH phases within the cementitious matrixes [2-6]. The most commonly used nanomaterials in cementitious products are nanoscale particles like silica-nanoparticles (SNP), Al_2O_3 (NA), TiO_2(NT), ZnO(NZ), Fe_2O_3(NF), clay nanoparticles (CNP) and carbon nano-tubes [7–9]. Clay nanoparticles are inexpensive raw materials that improve the microstructure of the cement composite [10-12]. A feature of CNP is its platelet form having a thickness of 1 nm and width of 70 to 150 nm. The uses of CNP in concrete may enhance the mechanical properties in cementitious composites by decreasing the porosity and pore size of the cement matrix [13, 14]. It was found that pastes containing 4, 6 and 10 % CNP showed higher compressive strength values [15, 16]. It has been postulated that the filling effect of CNP contributes the strength development and the pozzolanic reaction starting within 3 - 7 days [17].

The previous study also showed that the CH content of a cement paste with 10 % CNP decreased up to 42 %, this was attributed to the pozzolanicity of CNP, so that CNP improves the texture of the hydration products of the cement pastes and results in a quite dense, compact and uniform microstructure [15, 18].

Mineral admixtures such as fly-ash (FA), silica fume (SF) and fine blast furnace slag (FBFS) are waste inorganic materials that have pozzolanic and/or latent hydraulic properties, improve the properties of concrete [19]. The technological and economic benefit use of these waste inorganic materials, as a partial replacement

in concrete include the improvement of the impermeability, chemical durability, thermal behaviour and enhance the strength. The partial replacement of waste inorganic materials may reduce the early strength, later strength, microstructure and durability of the concrete [20].

Bohá, *et al.,* [21] stated that fine slag offers various technological, economical, and environmental advantages, where it has significantly lower CO_2 emissions in comparison with OPC. Subsequently, it is more actively used as an admixture for concrete. Fly ash is also utilised as a by-product of industrial manufacturing processes. Fly ash is the residue from burning coal in power plants, which has glassy spherical particles.

The present research is aimed at studying the effect of clay nanoparticles on the mechanical properties and microstructure of blended cement-pastes.

EXPERIMENTAL

The starting materials used in this study were OPC, FBFS, FA and clay nanoparticles (CNP). The chemical analyses of these materials were investigated by XRF spectrometry as shown in Table 1. The clay nanoparticles were calcined at 750 °C/2 hrs. The XRD pattern of the raw CNP is shown in Figure 1. The superplasticiser-based polycarboxylate (SP) is an opaque light-yellow liquid with a density of 1.08 g·ml^{-1}.

The batch composition based on the aforementioned starting materials are tabulated in Table 2. The CNP and SP were stirred with a suitable W/C ratio (standard consistency) as given in Table 2, at speed of 120 rpm for two min; the anhydrous blends (OPC, FBFS and/or FA) were mixed to full homogenisation at 90 rpm up to 2 min and homogenised in a rotary mixer at 120 rpm up to 30 s; then the cement blends were allowed to rest for 90 s; this was followed by mixing at 120 rpm for 1 min, then the blended pastes were cast into 2.5 × 2.5 × 2.5 cm^3 moulds, and then stored in a humidity cabinet (100 % RH) at 23 ± 1 °C for 24 hrs and then stored under water until the required time of testing (1, 3, 7, 28, 90 and 360-days).

The consistency and STs of the fresh mixed blends were monitored according to ASTM: C191 [22]. The hydrated pastes were stopped using a methanol-acetone mixture, and diethyl ether, and then dried at 70 °C up to 1 h [23]. The chemically combined water content (Wn), free lime (FL), bulk density (BD) and total porosity (TP) were determined as described in previous research [24, 25]. The compressive strength was calculated after the determination of the BD and TP according to the ASTM specifications (C-150) [26]. Some selected hydra-ted samples were examined using XRD, DTG/TGA and SEM techniques to verify the mechanism predicted by the chemical and mechanical tests. For the XRD analysis, a Philips X-ray Diffractometer of Cu Kα radiation (λ = 1.5418 Å) was used (model PW 1730). The speed of the scan was 2θ/min between 5° - 65°. The X-ray tube voltage was 40 kV and the current was 25 mA. The XRD analysis was performed with computer software searching for the PDF diffraction data. The TGA/DTG analysis was performed by using a Shimadzu DSC-50 thermal analyser at a heating rate of 10 °C·min^{-1}, the rate flow of nitrogen was 30 cm^3·min^{-1}. The microstructure of the OPC and some other selected cement pastes were investigated by Scanning Electron Microscope (SEM).

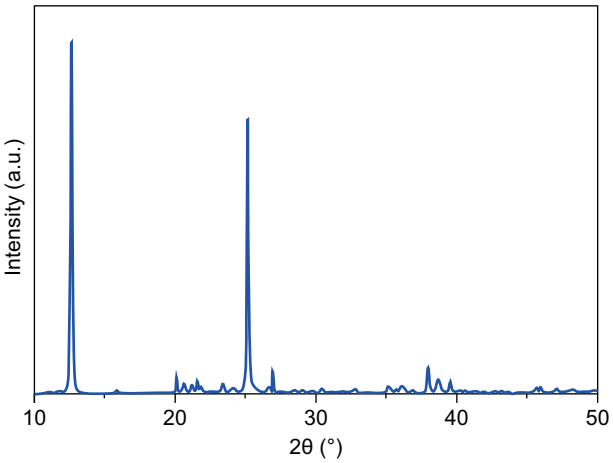

Figure 1. The XRD pattern of the raw CNP.

Table 2. The composition of the different mixes (mass %).

Mix	OPC	FA	FBFS	CNP	SP
C0	100	0	0	0	1
C1	94	0	0	6	1
C2	60	40	0	0	1
C3	54	40	0	6	1
C4	60	0	40	0	1
C5	54	0	40	6	1
C6	54	20	20	6	1
C7	34	20	40	6	1

Table 1. The chemical analyses of the OPC, FBFS, FA and CNP (mass, %).

	SiO_2	Al_2O_3	Fe_2O_3	CaO	MgO	SO_3	Na_2O	K_2O	LOI	Total
CNP	61.24	20.89	5.38	0.16	0.38	0.17	0.71	0.61	10.62	99.99
FBFS	43.21	9.97	0.59	35.96	5.43	1.37	0.79	0.67	1.98	99.97
FA	63.10	26.54	5.4	2.33	0.01	0.09	0.85	0.52	0.8	99.64
OPC	21.3	3.58	5.05	63.48	1.39	2.05	0.26	0.22	2.57	99.90

RESULTS AND DISCUSSION

Water consistency, initial, and final setting times

The mixed and design patches of the starting materials are represented in Figure 2. The results show that the CPC pastes containing CNP need excess water for consistency and have shorter setting times when compared with the neat cement paste. The CPC containing CNP was homogenised by a considerable amount of consistency for good workability, in addition to the presence of SP, leading to increases in the fluidity of the fresh CPC; therefore, the CPC cement pastes possess high hydraulic characteristics, followed by an acceptable setting time when compared with the blank cement paste. This may be due to the acceleration of the ettringite formation and the CSH, CAH and CASH hydrated gel products by the added CNP [27-31].

The results showed that the consistency of CPC-pastes containing FBFS are lower than those of the CPC-cement containing the FA-composite. It was found that the FA-composite cement paste containing FA was homogenised with a high amount of consistency and gives longer setting times, this is attributed to the lower activity of the FA than the FBFS. On the other hand, the cement containing FBFS showed lower consistency, while the setting times were reduced. It was concluded that mix C5 showed the lowest setting times when compared with all the cement mixes, this may be due to the formation as mentioned before. The STs of the CPC-pastes containing CNP accelerated in the existence of CNP [27]. The results also show that the consistency of mixes C6 and C7 decreases, whereas the STs elongated, this is due to the reduction of the OPC-content, as shown in Figure 2.

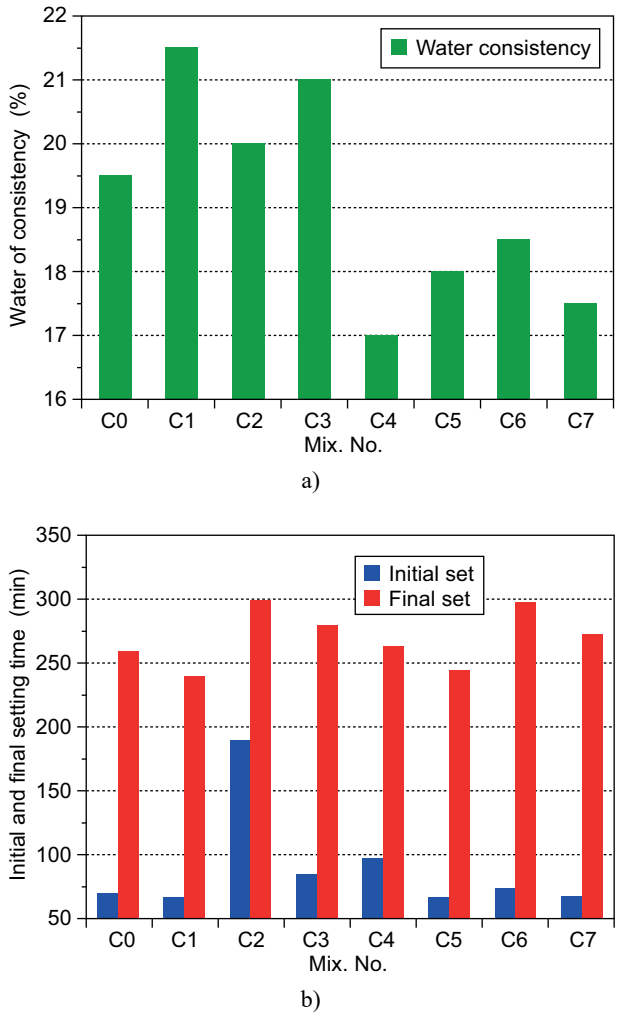

Figure 2. The consistency, setting times of the CPC with and without 6 % CNP.

Free lime contents

Figures 3 represents the free lime content (FL) of the cement composite pastes containing the CNP after 360 days of curing. From Figure 3, it can be found that all the CPC-pastes mixes showed a decreasing trend, while the blank cement paste (OPC) showed an increasing trend from day 1 up to day 360, respectively. All the CNP mixes cured after 3 days showed a slight decrease in the FL content. For the blank OPC cement paste (mix C1), during all the curing ages of the hydration reaction, it liberates excess $Ca(OH)_2$ (CH) while the addition of CNP acts as a promotor, which accelerates the pozzolanic reaction which means decreasing the CH by formation of CSH, CAH and CASH gel hydrates [32, 33]. For the mixes containing FA, FBFS and CNP, which showed a synergetic effect to enhance the pozzolanic reaction performance, leads to a decrease in the free lime contents.

The results show that the FL content of the OPC paste increases with the age up to 360 days, which is attributed to the continued hydration reaction, liberating the CH through the hydration period. The presence of CNP tends to decrease the residual portlandite, due to the pozzolanic interaction of the CNP with the portlandite leading to the formation of CSH, CAH and CASH

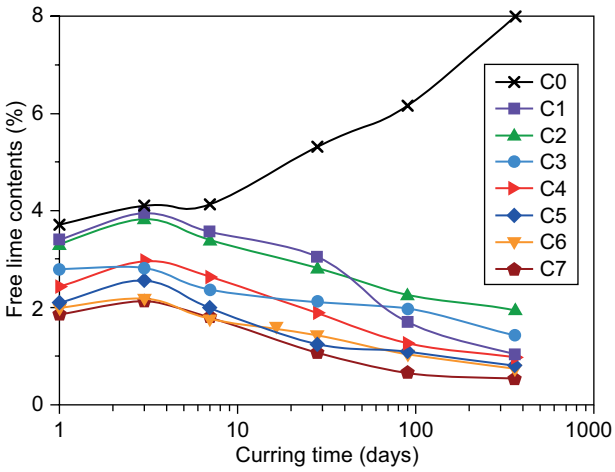

Figure 3. FL of the composite pastes with and without 6 % CNP.

hydrated gel products [32, 33]. The presence of CNP, leading to the raising of the FL content to 3 days due to the enhances in the hydration reaction OPC (lime production), and then decreases up to 360 days where the rate of consumption of the CH is higher than the rate of liberation due to higher pozzolanic activity of the CNP (lime consumption). The occurrence of SP tends to approach the CNP particles from the liberated lime to form further CSH, CAH and CASH, which precipitated in the vacant pore-system; hence, the porosity decreases as shown later. Mix C7 showed lower values than mixes C6 and C5.

Chemically combined water contents

The chemically combined water content (W_n) of the different CPC mixes is illustrated in Figure 4. All the mixes showed increasing trends all over the curing ages. The mixes containing 6 mass % CNP have higher W_n values in comparison with the neat-OPC paste. The hydration reaction of the OPC cement phases and the pozzolanic reaction is considered to be the main reason for this increase, the presence of CNP promotes the pozzolanic reaction via the formation of many hydrated phases like CSH(I) and CSH(II) with a considerable quantity, which is responsible for increasing the chemically combined water content.

The results show that the pozzolanic action of the FA is lower than that of the FBFS, the FA-composite-cement-pastes have lower W_n values than the FBFS-CPC-cement-pastes. The results also show that the chemically combined water content increases by increasing the content of the FBFS, where mix C7 has higher W_n values than mix C6, especially at the early ages of hydration, this may due to the pozzolanic reaction of the FBFS, the CNP with the liberated CH from the OPC cement hydration, which enhances the later hydration times [34, 35].

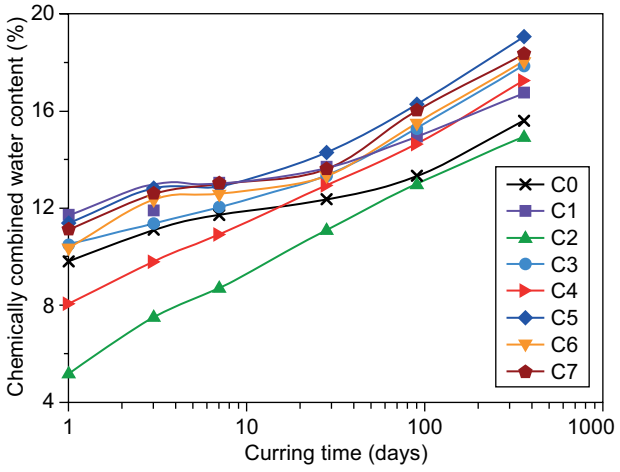

Figure 4. The Wn of the CPC pastes with and without 6 % CNP.

Compressive strength

The compressive strength (CS) of the composite-pastes containing 6 % CNP up to 360-days is illustrated in Figure 5. The data obtained from Figure 5 represent an increase in the CS with an increase in the age-period for all the hardened pastes, qualified to the formation of a successive amount of CSH, CAH and CASH as the main source of strength, these hydrates precipitated in the accessible vacant pores to form a closed compact body [30]. The inclusion of 6 mass% CNP gives a higher CS than pastes without the CNP (Figure 5), ascribed to the formation of micro- and nano-sized hydrates in the cementitious matrix. The CS of the composite-cement-pastes showed better-quality in the presence of 6 % CNP for all the CPC pastes containing FA and/or FBFS; this is due to the pozzolanic reaction of the CNP and the free CH liberated during the OPC hydration production [36].

Figure 5 shows that the CS of mix C5 is higher than the FA-CPC pastes (mix C3) this is attributed to the pozzolanic activity of the hybrid CNP and FBFS, which worked to develop the hydration process of the CPC, especially at the later hydration times. The data also, showed that the CS of mix C7 had higher values than mix C6, due to the pozzolanicity of the FBFS and CNP.

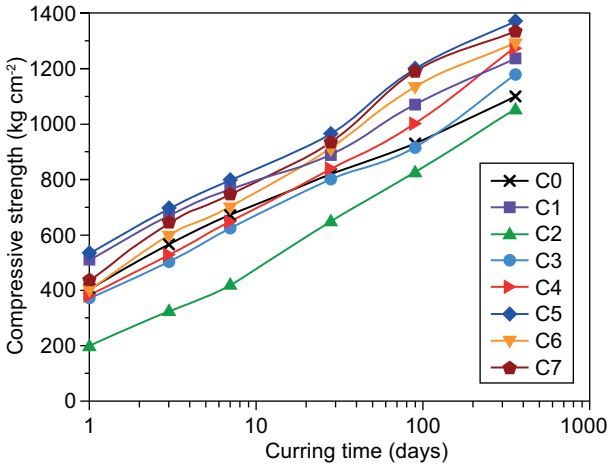

Figure 5. The CS of the composite pastes with and without 6 % CNP.

Gel/space ratio (X)

The gel/space ratio (X) of the CPC-pastes containing FA, FBFS and 6 % CNP is demonstrated in Figure 6. The gel/space ratio was influenced by the W/C ratio, hydration of degree, porosity, and curing-age and temperature. The X-ratio increases with the age for all the cement pastes, this is due to the formation of large amounts of CSH, CAH and CASH products [37]. The presence of SP, W/C and TP decrease so that the X values increase [34]. The results showed that mix C5

show a higher gel/space ratio value in comparison with mix C3, due to the presence of 6 % CNP, which activates the reaction of the FBFS to give a higher CS and an *X*-ratio as shown in Figures 5 and 6. The represented results showed that the gel/space ratio increased by the FBFS content (mixes C7 and C6). Mix C7 showed higher gel/space ratio values than C6, this demonstrates that 40 % of the FBFS is more suitable than 20 % of the FBFS which gives more hydration products.

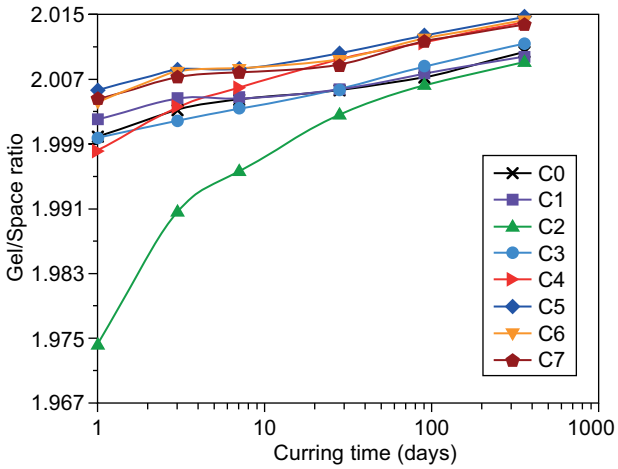

Figure 6. The gel/space ratio of the pastes containing 6 mass % CNP.

Bulk density (BD) and total porosity (TP)

The values of the bulk density (BD) and the total porosity (TP) of the CPC-pastes in the existence of 6 % CNP and the SP in the hybrid effect treated up to 360 days are tabulated in Table 3. The BD increases wherever the TP decreases with the treatment ages, this is accredited to the increases in the excessive hydration products. These products act as binding centres amongst the unhydrated and hydrated phase fractions of the CPC-grains through the progressive hydration, hence the TP decreased. The gel/space ratio and the bulk density increase in addition, the total porosity decreases. The BD cement composite pastes containing CNP represents higher values than the neat paste and/or the other CPC mixes lacking the CNP [30]. The BD of mix C5 has higher values than those of the neat-paste and mix C3, especially at later hydration ages. By increasing the content of the FBFS up to 40 %, the BD increases and the TP decreases. From the derived results, it can be concluded that the physico-mechanical properties, namely the CS, gel/space ratio, TP, and BD are in good agreement with each other and they represent an increasing trend, except for the TP, which showed a decreasing trend from 1 day up to 360-days.

XRD patterns

Figure 7 represents the X-ray diffraction patterns of the hardened CPC pastes namely the C0, C3, C5, C6 and C7 mixes treated at 1 day and 90 days. Figure 7 represents the hydrated and anhydrate-phase diffraction lines of the CH, β-C_2S, C_3S, C, CSH and quartz as shown in Figure. 7. The diffraction lines are consistent to the C0 mix exhibiting higher intensities as represented for the portlandite diffraction lines.

As the hydration-proceeds, the intensity of the peak, illustrating the diffraction patterns of the CSH, increased, whereas the diffraction patterns corresponding to the CH decreased from one-day up to 90 days, as represented in the composite pastes containing CNP (mixes C3 and C5). This is due to the pozzolanic reaction between the CNP with the lime liberated during the hydration reaction of the cement, leading to the higher consumption of portlandite and the formation of further C–S–H. Increasing the content of the FBFS-FA-CPC pastes, the peaks characteristic to the portlandite and calcite phases decreased; this is due to lowering the content of the OPC.

Table 3. The bulk density and total porosity of the composite pastes in the presence of 6 mass % CNP.

Time (days)	Bulk density (g·cm^{-3})							
	C0	C1	C2	C3	C4	C5	C6	C7
1	2.146	2.267	2.002	2.200	2.172	2.249	2.235	2.245
3	2.178	2.301	2.074	2.239	2.181	2.275	2.251	2.266
7	2.197	2.324	2.114	2.247	2.191	2.321	2.275	2.312
28	2.226	2.349	2.181	2.261	2.223	2.346	2.302	2.354
90	2.252	2.367	2.205	2.273	2.267	2.384	2.341	2.381
360	2.288	2.410	2.232	2.299	2.311	2.421	2.379	2.401
Time (days)	Total porosity (%)							
	C0	C1	C2	C3	C4	C5	C6	C7
1	31.24	28.45	32.24	30.21	29.43	28.16	29.07	29.60
3	30.01	27.96	31.76	29.31	28.39	27.83	28.67	29.00
7	29.21	26.93	30.96	28.19	27.19	26.62	27.06	28.10
28	28.65	25.94	29.45	27.43	25.75	25.75	26.21	27.30
90	27.11	24.60	28.04	26.22	24.01	24.11	24.79	26.10
360	25.47	23.08	26.14	24.46	22.69	22.48	23.10	24.30

This result is in good agreement with the results of the compressive strength and the gel/space ratio.

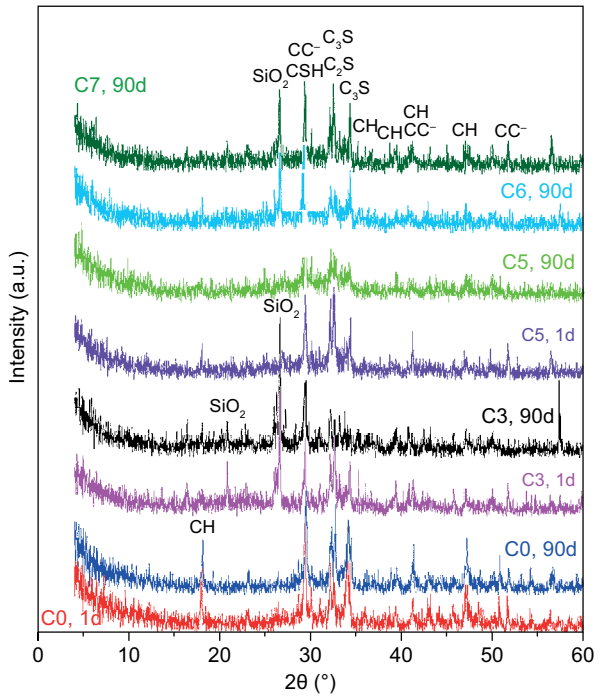

Figure 7. The XRD patterns of the CPC-pastes cured at 1 day, 90 days.

TGA/DTG thermograms

The TGA/DTG thermograms of the OPC and composite pastes containing 6 % CNP and 1 % SP cured at 1 day and 90 days are represented in Figure 8. The DTG/TGA curves show the typical temperature events up to 1000 °C. The peaks presented at 80 – 190 °C are attributed to the decomposition of the calcium silicate hydrate, tri-sulphoaluminate hydrate (AFt), and/or monosulphate-hydated products (AFm). The peak situated at 120 - 190 °C is related to the dehydration of the CSH in the different crystalline states, which overlapped with the Aft, AFm and CASH hydrates [38]. However, the peak situated at 450 - 525 °C is interrelated to the dehydroxylation of CH [39, 40]. The endothermic peaks detected at 680 and 720 °C are accredited to the calcination of the amorphous and crystalline $CaCO_3$ (C) [41]. The exothermic peak located at 850 - 950 °C is due to the recrystallisation of the monocalcium silicate, which is produced from the pozzolanic reaction [42]. Figure 8A illustrates the TGA/DTG thermograms of the C0 mix hydrated for 1 day and 90 days, it can be deduced that the areas under the peaks corresponding to the C-S-H and CH phases increase with the treatment ages. Whereas the addition of CNP to the FA and/or FBFS CPC-paste leads to an increase in the area under the peak identical to CSH and used up the CH in its pozzolanic action, hereafter, the area under the peak identical to the CH decreases when compared with the neat paste as shown in Figure 8B and 8C.

Microstructure and morphology of cement paste composites

The SEM micrographs of the selected cement com-posite mixes C3, C5, C6, and C7 are represented in Figure 9a-e. From Figure 9a-e, it was found that the sample C3 cured after 90 days of hydration showed

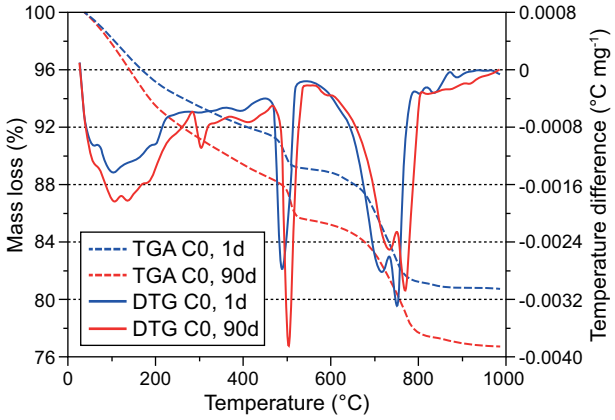

a)

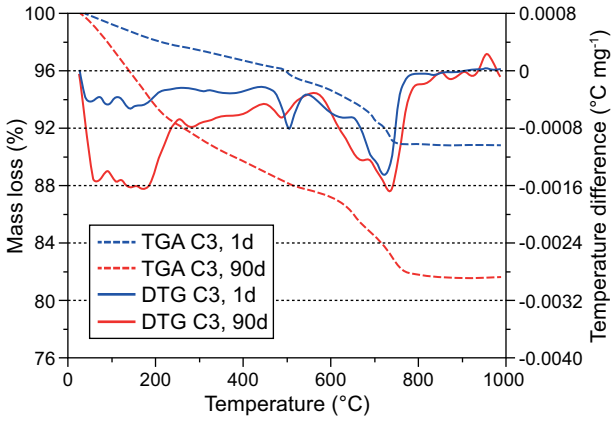

b)

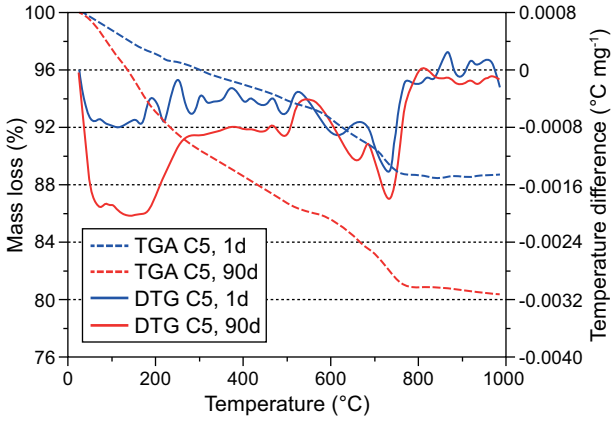

c)

Figure 8. The consistency, setting times of the CPC with and without 6 % CNP.

a denser structure, which is mainly composed of the fully nano-crystalline hydration products and rod like particles of the CSH (Figure 9a). The dense structure may be due to the effect of the CNP particles' nucleus, which accelerates the pozzolanic activity leading it to form a homogenous compact CPC.

The SEM micrograph of mix C5 treated after 90 days depicts a porous microstructure with wider pores available for the crystallisation of the formed CSH, CAH, CASH. These microstructures exhibit a higher degree of crystallinity of a mineral hexagonal form of gehlenite like hydrate (C_2ASH_8), the pore size decreases due to the higher activity of the CNP as shown in Figure 9b. This microstructure reflects the higher compressive strength values, which promotes a decrease in the free lime by the formation of the CSH, CAH, CASH phases [43-45].

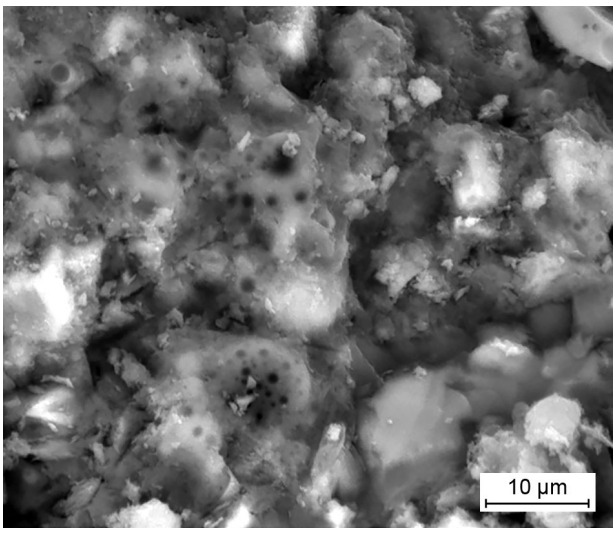

a)

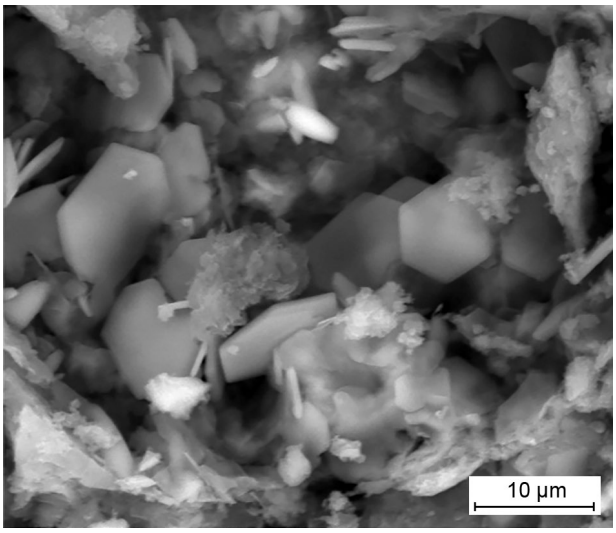

b)

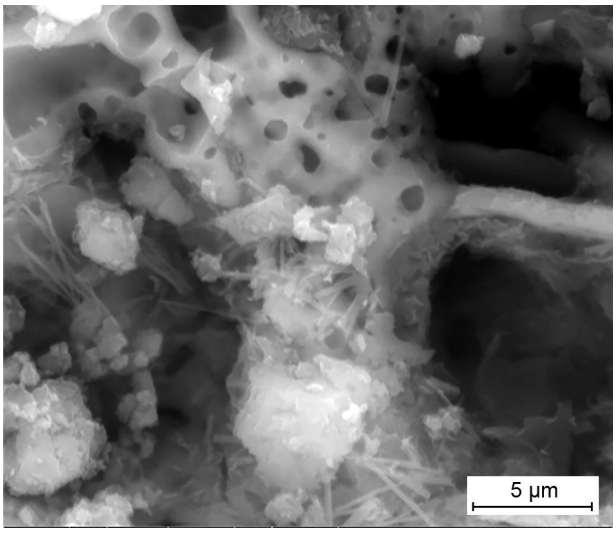

d)

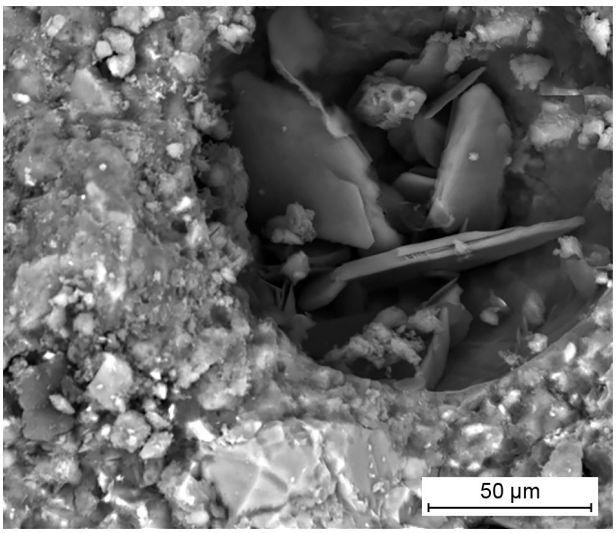

c)

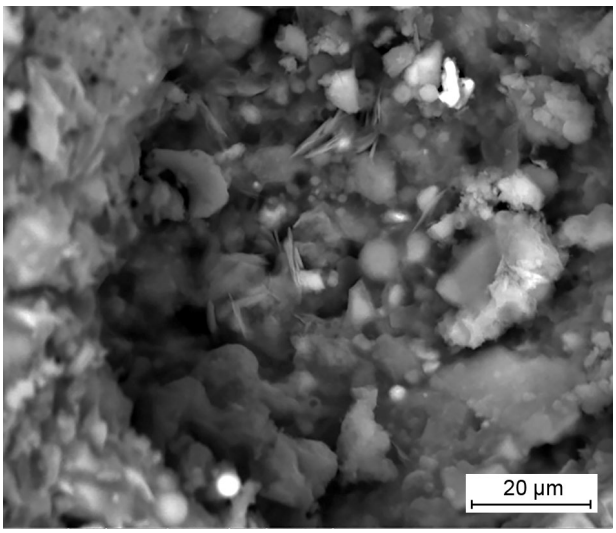

e)

Figure 9. The SEM micrographs of the composite cement pastes; a) C3-90d; b) C5-90d; c) C6-90d with 50µm magnification; d) C6-90d with 10µm magnification; e) C7-90d.

Figure 9c and 9d represent the micrographs of the hardened cement paste composite C6 with different magnifications treated at 90 days. The SEM micrograph of mix C6 displayed the presence of C–S–H and CH as the main hydrated products in addition to the presence of C–A–H, C_2ASH_8 and C_3AH_8. The microstructure of mix C6 is a heterogeneous structure where it contains different types and number of pores when compared with mix C5. This microstructure reflects the variation of both the compressive strength, bulk density and porosity.

Figure 9e represents the micrograph of C7, the microstructure represents the flaky plate-like morphology of C_2ASH_8. It also shows the presence of ill-crystalline and microcrystalline hydrates of C–S–H with the complete disappearance of $Ca(OH)_2$. After 90 days of hydration, more hydrated products were placed in the pores where the denser structure is obtained. The micrograph also shows longer rod-like formations of C–S–H. This CSH phase is in a large quantity, which is responsible for bridging the cement particles, producing a rigid closed compact structure.

CONCLUSIONS

It can be concluded that:

- The results show that the CPC pastes containing CNP need excess water for consistency and shorter setting times when compared with the neat cement paste. The STs of the CPC-pastes containing CNP accelerated in the existence of the CNP. The results also show that the consistency of mixes C6 and C7 decreased, whereas the STs elongated.
- The free lime content of the CPC-pastes mixes showed a decreasing trend, while the OPC showed increasing trends from 1 day up to 360 days. The mixes containing CNP showed a synergetic effect with the FA and the FBFS to enhance the pozzolanic reaction performance forming further CSH, CAH and CASH, which precipitated in the vacant pore-system producing a compact matrix; hence, the compressive strength, gel/space ratio, bulk density and chemically combined water increased, whereas the porosity decreased.
- The microstructure of the CPC represented the presence of the flaky plate-like morphology of C_2ASH_8 as well as the ill-crystalline and microcrystalline hydrates of C-S-H with the complete disappearance of $Ca(OH)_2$. This CSH phase is responsible for bridging, producing a rigid closed compact structure.

REFERENCES

1. Yang H., Cui H., Tang W., Li Z., Han N., Xing F. (2017): A critical review on research progress of graphene/cement based composites. *Composites Part A: Applied Science and Manufacturing*, *102*, 273-296. doi: 10.1016/j.compositesa.2017.07.019
2. Nik A.S., Bahari A. (2012): Nano-particles in concrete and cement mixtures. *Applied Mechanics and Materials*, *110*, 3853–3855. doi: 10.4028/www.scientific.net/AMM.110-116.3853
3. Norhasri M.S.M., Hamidah M.S., Fadzil A.M. (2017): Applications of using nano material in concrete: A review. *Construction and Building Material, 133*, 91–97. doi: 10.1016/j.conbuildmat.2016.12.005
4. Amin M. S., Abo-El-Enein S. A., Abdel Rahman A., Alfalous K. A. (2012): Artificial pozzolanic cement pastes containing burnt clay with and without silica fume: physicochemical, microstructural and thermal characteristics. *Journal of Thermal Analysis and Calorimetry*, *107*(3), 1105-1115. doi: 10.1007/s10973-011-1676-5
5. Montes O.B., Palacios M., Rivilla P., Puertas F. (2012): Compatibility between superplasticizer admixtures and cements with mineral additions. *Construction and Building Material, 31*, 300–309. doi: 10.1016/j.conbuildmat.2011.12.092
6. Aye T., Oguchi C.T. (2011): Resistance of plain and blended cement mortars exposed to severe sulfate attacks. *Construction and Building Material, 25,* 2988–2996. doi: 10.1016/j.conbuildmat.2010.11.106
7. Han B., Sun S., Ding S., Zhang L., Yu X., Ou J. (2015): Review of nanocarbon-engineered multifunctional cementitious composites. *Composites Part A: Applied Science and Manufacturing*, *70*, 69-81. doi: 10.1016/j.compositesa.2014.12.002
8. Mukhopadhyay A. K. (2011). Next-generation nano-based concrete construction products: a review. In *Nanotechnology in Civil Infrastructure*. Springer, Berlin, Heidelberg, pp. 207-223. doi: 10.1007/978-3-642-16657-0_7
9. Shah S. P., Hou P., Konsta-Gdoutos M. S. (2016): Nano-modification of cementitious material: Toward a stronger and durable concrete. *Journal of Sustainable Cement-Based Materials*, *5*(1-2), 1-22. doi: 10.1080/21650373.2015.1086286
10. Hakamy A., Shaikh F. U. A., Low I. M. (2015).: Characteristics of nanoclay and calcined nanoclay-cement nanocomposites. *Composites Part B: Engineering*, *78*, 174-184. doi: 10.1016/j.compositesb.2015.03.074
11. Aly M., Hashmi M. S. J., Olabi A. G., Messeiry M., Hussain A. I. (2011): Effect of nano clay particles on mechanical, thermal and physical behaviours of waste glass cement mortars. *Material and Science Engineer, 528,* 7991–7998. doi: 10.1016/j.msea.2011.07.058
12. Alamri H., Low I. M., Alothman Z. (2012): Mechanical, thermal and microstructural characteristics of cellulose fibre reinforced epoxy/organoclay nanocomposites. *Composites Part B: Engineering*, *43*(7), 2762-2771. doi: 10.1016/j.compositesb.2012.04.037
13. Wei J., Meyer C. (2014): Sisal fiber-reinforced cement composite with Portland cement substitution by a combination of metakaolin and nano-clay, *Journal of Material Science, 49*, 7604–7619. Doi: 10.1007/s10853-014-8469-8
14. Taha S. (2010): Thermo–Mechanical Properties of Activated Nano Clay Cement Pastes at Different Curing Temperatures. In: International Conference on Nano Technology for Green and Sustainable Construction, Cairo, pp. 14-17.
15. Morsy M. S., Alsayed S. H., Aqel, M. (2010): Effect of nano-clay on mechanical properties and microstructure of ordinary Portland cement mortar. *International Journal of Civil & Environmental Engineering IJCEE-IJENS*, *10*(01), 23-27.

16. Supit S. W. M., Rumbayan R., Ticoalu A. (2017): Mechanical properties of cement concrete composites containing nano-metakaolin. *AIP Conference Proceedings, 1903*, 050001. doi: 10.1063/1.5011540
17. Norhasri M. M., Hamidah M. S., Fadzil A. M., Megawati O. (2016): Inclusion of nano metakaolin as additive in ultra high performance concrete (UHPC). *Construction and Building Materials*, *127*, 167-175. doi: 10.1016/j.conbuildmat.2016.09.127
18. Shoukry H., Kotkata M. F., Abo-el-Enein S. A., Morsy M. S. (2013): Flexural strength and physical properties of fiber reinforced nano metakaolin cementitious surface compound. *Construction and Building Materials*, *43*, 453-460. doi: 10.1016/j.conbuildmat.2013.02.030
19. Kosmatka S.H., Panarese W.C. (1988). *Design and Control of Concrete Mixtures*. Skokie, IL, USA,Portland Cement Association, p. 17, 42, 70, 184.
20. Shi C., Qian J. (2000): High performance cementing materials from industrial slag. *Resources, Conservation and Recycling*, *29*, 195-220. doi: 10.1016/S0921-3449(99)00060-9
21. Boháč M., Palou M., Novotný R., Másilko J., Všianský D., Staněk T. (2014): Investigation on early hydration of ternary Portland cement-blast-furnace slag – Metakaolin blends. *Construction and Building Materials, 64*, 333–341. doi: 10.1016/j.conbuildmat.2014.04.018
22. ASTM C191 (2008). Standard method for normal consistency and setting of hydraulic cement.
23. Abd-El Aziz M.A., Heikal M., Abd El Aleem S. (2012): Physico-chemical and mechanical characteristics of pozzolanic cement pastes and mortars hydrated at different curing temperatures. *Construction and Building Material, 26*, 310–316. doi: 10.1016/j.conbuildmat.2011.06.026
24. Abd-El-Eziz M.A., Heikal M. (2009): Hydration characteristics and durability of cements containing fly ash and limestone subjected to Qaron's Lake Water. *Advanced Cement Research, 21*, 91–99. doi: 10.1680/adcr.2007.00025
25. El-Didamony H., Abd-El Eziz M., Abd El Aleem S., Heikal M. (2005): Hydration and durability of sulfate resisting and slag cement blends in Qaron's Lake water. *Cement and Concrete Research, 35*, 1592–1600. doi: 10.1016/j.cemconres.2004.06.038
26. ASTM C109 (2007). Strength test method for compressive strength of hydraulic cement mortars.
27. Badogiannis E., Kakali G., Tsivilis S. (2005): Metakaolin as supplementary cementitious material: optimization of kaolin to metakaolin conversion. *Journal of Thermal Analysis and Calorimetry*, *81*(2), 457-462. doi: 10.1007/s10973-005-0806-3
28. Sololev K., Nemecek J., Smilauer V., Zeman, J. (2009): Engineering of nano particals for optimal performance in nano cement based materials. In: Nanotechnology in Constr. Proc., Prague, pp. 139-148.
29. Li G. (2004): Properties of high volume of Fly ash concrete incorporating nano- SiO_2. *Cement and Concrete Research, 34*, 1043-1049. doi: 10.1016/j.cemconres.2003.11.013
30. Nazari A., Riahi S. (2011): The effects of SiO_2 nanoparticles on physical and mechanical properties of high strength compacting concrete. *Composites Part B: Engineering*, *42*(3), 570-578. doi: 10.1016/j.compositesb.2010.09.025
31. Heikal M., Aiad I., Shoaib M.M., EL-Didamony H. (2001): Physico-chemical characteristics of some polymer cement composites. *Materials Chemistry and Physics, 71*, 76-83. doi: 10.1016/S0254-0584(01)00346-7
32. Esteves L.P. (2011): On the hydration of water-entrained cement-silica system combined SEM, XRD and thermal analysis in cement pastes. *Thermochimica Acta, 518,* 27–35. doi: 10.1016/j.tca.2011.02.003
33. El-Diadamony H., Amer A. A., Sokkary T. M., El-Hoseny S. (2018): Hydration and characteristics of metakaolin pozzolanic cement pastes. *HBRC Journal*, *14*(2), 150-158. doi: 10.1016/j.hbrcj.2015.05.005
34. Khatib J.M., Hibbert J.J. (2005): Selected engineering properties of concrete incorporating slag and metakaoline. *Construction and Building Material, 19*, 460–472. doi: 10.1016/j.conbuildmat.2004.07.017
35. Deschner F., Winnefeld F., Lothenbach B., Seufert S., Schwesig P., Dittrich S., Goetz-Neunhoeffer F., Neubauer J. (2012): Hydration of Portland cement with high replacement by siliceous fly ash. *Cement and Concrete Research, 42,* 1389-1400. doi: 10.1016/j.cemconres.2012.06.009
36. Echart A., Ludwig H.M., Stark J. (1995): Hydration of the four main Portland cement clinker phases. *Zemenk-Kalk-Gips, 28*, 443–452.
37. Abd El-Aziz M., Abd El-Aleem S., Heikal M., El-Didamony H. (2004): Effect of Polycarboxylate on Rice Husk Ash Pozzolanic Cement. *Sil. Ind. 69,* 73-84.
38. El-Didamony H., Amer A.A., Helmy I.M., Mostafa K. (1996): Durability of sulphate resisting slag blended cements and mortars in sea water. *Indian Journal of Engineering and Materials Sciences (IJEMS), 3*, 35–40.
39. Esteves L.P. (2011): On the hydration of water-entrained cement–silica systems combined SEM, XRD and thermal analysis in cement pastes. *Thermochimica Acta, 518*, 27-35. doi: 10.1016/j.tca.2011.02.003
40. Wongkeo W., Chaipanich A. (2010): Compressive strength, microstructure and thermal analysis of autoclaved and air cured structural lightweight concrete made with coal bottom ash and silica fume. *Material Science Engineering, 527*, 3676-3684. doi: 10.1016/j.msea.2010.01.089
41. Vedalakshmi R. (2003): Quantification of hydrated cement products of blended cement in low and medium strength concrete using TG and DTG technique. *Thermochimica Acta, 407*, 49-60. doi: 10.1016/S0040-6031(03)00286-7
42. Ramachandran V.S. (2001). Thermal Analysis. In: *Handbook of analytical techniques in concrete science and technology*. Noyes publications, New Jersey.
43. Colston S.L., Connor D., Barnesm P. (2000): Functional micro-concrete: The incorporation of zeolites and inorganic nano-particles into cement micro-structures. *Journal of Materials Science Letters, 19*, 1085-1088.
44. Lia K., Chang P., Peng Y., Yang C. (2004): Study on characteristics of interfacial transition zone in concrete. *Cement and Concrete Research, 34*, 977-989. doi: 10.1016/j.cemconres.2003.11.019
45. Al-Salami A.S., Taha S., Shoukry H. (2013): Physico-mechanical characteristics of blended white cement pastes containing thermally activated ultrafine nano-clays. *Construction and Building Materials, 47*, 138-145. doi: 10.1016/j.conbuildmat.2013.05.011